Manuscript
Click here to download Manuscript: manuscript_jjlopez.doc
Click here to view linked References

Molecular Structure and Vibrational Spectra Analysis of Diethylsilanediol by IR and Raman spectroscopies and DFT calculations

M. P. G. Rodríguez Ortega[1], M. Montejo[1], A. Marchal Ingraín[2], F. Márquez[1], J. J. López González*[1]

[1]Physical and Analytical Chemistry Department, University of Jaén, Campus Las Lagunillas, E-23071, Jaén, Spain

[2]Inorganic and Organic Chemistry Department, University of Jaen, Campus Las Lagunillas, E-23071, Jaen, Spain.

Abstract

A thorough theoretical analysis (DFT/ B3LYP) of the potential energy surface (PES) of diethylsilanediol (DESD) allowed finding ten stable conformations of the molecule, differing on the relative arrangement of both ethyl and hydroxyl groups. The Boltzmann's population analysis allowed establishing their stability order that was justified in terms of the anomeric effect analyzed by means of the Natural Bond Orbitals (NBO) methodology. Besides, DESD was synthesized and characterized using FT-IR and Raman spectroscopies data, firstly reported in this work, combined with DFT calculations (B3LYP/ aug-ccpVTZ). Finally some of the main structural and vibrational features of this and other closely related alkylsilanediols, i. e. DMSD and EMSD, have been put together in order to establish some trends that can allow a better understanding of the chemistry of these compounds.

Keywords

Diethylsilanediol, IR, Raman, Structure, Vibrational spectra.

*Corresponding author:

jjlopez@ujaen.es

1 Introduction

Organosilicon compounds are a wide family with a large variety of applications in the chemical industry. Specifically, silanediols are important intermediates in sol-gel processes [1], aimed to obtain different oxidic materials (SiO_2 based) with tailored properties, such as ceramics, fibers, films, etc. Moreover, some related compounds containing the *gem*-diol group (silicon bioisosteres), have recently proven a biological role as inhibitors of aspartyl and metalloproteases [2,3]. However, the number of works dealing with the structural characterization of small *gem*-diol systems (such as the title compound) is scarce, partly due to their chemical instability revealed by their accused tendency to policondensation (which decreases with the increasing size of the alkyl side chains) giving the corresponding siloxanes.

Few works can be found in the literature concerning the study of diethylsilanediol (DESD). The first one dates from 1946 [4] in which George *et al.* describe the synthesis of DESD *via* the hydrolysis of dichloro(diethyl)silane. The crystal structure of the DESD molecule was studied some years later (in 1953) by Kakudo *et al.* [5] The same year George *et al*. reported, for a second time, the synthesis of DESD using several hydrolysis methods. [6] The crystal structure was once again evaluated by X-ray diffraction by Tomlins *et al.* in 1985. [7]

Although, as mentioned above, the synthesis and structural characterization (X-ray) of DESD was accomplished before, the vibrational spectra of the species (which can be of interest for the monitoring of the sol-gel reactions in which it takes part) has not been studied, neither theoretically nor experimentally. Thus, our principal target has been to achieve a better description of the structural and spectroscopic properties of the silanediol group in a relatively simple chemical environment (a relatively small alkyl *gem*-diol). DFT calculations have allowed a complete structural and conformational analysis of the title compound (ten molecular conformations represent minima in the PES of the molecule). The following study of the electronic structure of all the conformers, by means of NBO population analysis, has provided a better insight on their stability order and molecular features on the basis of the anomeric effect. Besides, with the support of quantum chemical calculations, the firstly recorded IR and Raman spectra of the species have been thoroughly analyzed and completely assigned. Finally, the most interesting features of the molecular structure and vibrational spectra of the species and two other structurally related silanediols, i.e. dimethylsilanediol (DMSD),

and ethylmethylsilanediol (EMSD), are jointly reported in order to perform a comparative analysis. The results obtained would help to carry out the subsequent study of bigger and more complex systems.

2 Experimental Details

2.1. Synthesis

DESD was prepared in 74% yield from commercial dichloro(diethyl)silane using the procedure reported by *Cella et al.* [8]. This is a modified procedure of the previously reported Takiguchi's procedure [9] which allows the obtaining of silanediol more stable to storage for months in freezer without deterioration than using Takiguchi's. This aspect is noteworthy due to the high propensity of the silanediols to undergo self-condensation depending on the synthetical conditions. ^{1}H NMR (400 MHz, DMSO-d_6, 25ºC) δ(ppm): 5.63 (s, 2H, OH); 0.87 (t, *J*=7.9Hz, 6H, $2CH_3$); 0.37 (q, *J*= 8.0Hz, 4H, $2CH_2$); ^{13}C NMR (100MHz, DMSO-d_6) δ(ppm): 6.76 ($2CH_3$); 6.54 ($2CH_2$).

2.2. Vibrational Spectra

IR spectra of the samples in solid phase were recorded in two different ways, i.e. using KBr pellets and thin films. For the preparation of the thin film, 20 μL of a solution of diethylsilanediol in acetone (0.05M) were deposited in a CsI disk. Afterwards, the solvent was evaporated under anhydrous conditions. IR spectra of the thin film were recorded in the 400-4000 cm^{-1} range using a FT-IR Jasco 4100 spectrophotometer, equipped with a Globar source and DTGS detector. IR spectra of the sample in KBr pellet was recorded in 300-4000 cm^{-1} range using a FT-IR Bruker Vector 22 spectrophotometer, equipped with a Globar source and a DTGS detector. Both spectra were obtained with a resolution of 1cm^{-1} and after 100 scans.

The Raman spectra of the pure solid were recorded with a Bruker RF100/S FT-Raman spectrometer, equipped with a Nd:YAG laser (excitation line 1064 nm) and a cooled Ge detector at liquid nitrogen temperature. The spectra were obtained with a resolution of 1 cm^{-1} and 100 scans.

3 Computational Details

DFT calculations were performed using the Gaussian 03 suite of programs [10]. Geometry optimizations and frequency calculations for the different conformers of DESD were carried out using the Becke's three-parametric hybrid exchange functional [11] combined with the Lee-Yang-Parr correlation functional (B3LYP) [12] in conjunction with the 6-31G* [13], 6-311++G** [14], and aug-cc-pVTZ [15] basis sets. Geometry optimizations convergence criteria were tighten using the keywords

opt=VTight, SCF=Tight and Int=Ultrafine, which minimize the threshold of the RMS value during the optimization process. The theoretical vibrational spectra of each stationary point obtained were calculated at the same level of theory in order to characterize them as real minima on the PES of the molecule.

The force fields obtained in Cartesian coordinates at the B3LYP/ aug-cc-pVTZ level were transformed into a set of natural internal coordinates [16] in order to obtain a more comprehensive description of the PEDM (Potential Energy Distribution Matrix). The force field transformation into natural valence coordinates and normal-mode analyses were performed using the MOLVIB [17,18] program.

Natural bond orbital NBO [19] calculations were accomplished using the NBO v3.1 [20] as implemented in Gaussian 03.

4 Results and discussion

4.1. Theoretical conformational Analysis and molecular structure

Conformational search of DESD was carried out considering the most stable orientation of both ethyl groups in the molecule according to their possible arrangements (i.e. *gauche* (*g+* or *g-*) and *anti* (*a*)) respect to the Si-O bonds, in which the C-C-Si-O dihedral angle can adopt approximately values of +60º, -60º and 180º, respectively. Eclipsed conformation of ethyl groups were discounted since they have much higher energy. The relative orientation of the hydroxyl groups was also evaluated performing a relaxed scan (B3LYP/ 6-31+G*) of the C-Si-O-H dihedral angle for each possible arrangement of the ethyl groups. As was previously found for the related systems dimethylsilanediol (DMSD) [21] and ethylmethylsilanediol (EMSD) [22], two different orientations of the OH groups have been observed in DESD. The most stable refers to a *gauche-gauche* (*gg*) conformation in which the OH groups are slanted from the OSiO plane by about 60º. The other one, which is (on average) 1.75 kcal/mol higher in energy than the first one, correspond to a *gauche-trans* (*gt*) arrangement of the hydroxyl groups being the dihedral angle H-O-O-H approximately 80º. Remarkably, this (*gt*) arrangement of the $Si(OH)_2$ resembles that obtained from the X-Ray analysis of the crystalline structure of DESD. [7] Figure 1 shows a schematic representation of the so-called (*gg*) and (*gt*) arrangement of hydroxyl groups in this sort of compounds.

All of these structures characterized by means of the computation of their vibrational spectra at the above mentioned level of theory. Consequently, ten different molecular conformations were found to be real minima on the PES of DESD (no imaginary vibrational frequencies were calculated for them). Molecular structures, atom

numbering and the main geometrical parameters obtained theoretically at the B3LYP/ aug-cc-pVTZ level for the whole set of conformers of DESD are shown in Figure 2.

The theoretical values of the main geometrical parameters calculated (B3LYP/ aug-cc-pVTZ) for the set of conformers of DESD, along with those obtained at the same level of theory for conformers of DMSD and EMSD are shown in Table 1. As can be seen, geometries of all the (*gg*) conformers are rather similar. In general, Si-O bond lengths are *ca*. 166.8 pm and the OSiO angles are approximately 110.7º (on average). In contrast, for (*gt*) conformers one of the Si-O bonds distances (denoted as SiO_2 in Table 1) is calculated *ca*. 1pm longer than the other (called SiO_3). Moreover, for this second set of conformers the OSiO angles are fairly smaller in comparison to their counterparts (*gg*).

The considerable shortening in bond distances in X-Ray results may be due to packaging effects in the solid phase.

Thus, the (*gt*) arrangement of the hydroxyls groups induces important changes in the molecular structures. For instance, focusing on DESD conformers, whereas in conformer IV both Si-O and both Si-C bond distances are almost the same, for structurally related conformer VIII Si-O_2 bond length is sensibly larger than Si-O_3 bond distance. The same goes for Si-C distances, being Si-C_5 larger than Si-C_4. This fact is observed in all pairs of conformers, and was also noticed for conformations found in DMSD and EMSD as can be seen in Table 1, where the averaged Si-O and Si-C bond distances of (*gg*) and (*gt*) conformers of DMSD, EMSD and DESD are reported.

These mentioned disparities in the geometrical parameters were understood to be a consequence of the electronic delocalization derived from the anomeric effect. As was stated previously for other close alkylsilanediol systems [21,22], the stabilizing anomeric effect is favored when OH groups are oriented in *gauche* arrangement. NBO analysis was carried out over the series of conformers in order to evaluate it.

Table 2 shows the electronic populations of the so-called lone pairs orbitals of the oxygen atom O_2 and O_3 along with the bonding σ and antibonding σ^* orbitals of the Si-O and Si-C bonds. In the NBO scheme, high populations of the antibonding σ^* orbitals are related with the lengthening of the bond distances. Comparing the electronic population of the antibonding orbitals $\sigma^*_{Si\text{-}O2}$ and $\sigma^*_{Si\text{-}O3}$, and $\sigma^*_{Si\text{-}C4}$ and $\sigma^*_{Si\text{-}C5}$ of conformers VII, VIII, IX and X, it can be seen that, unlike the remaining conformers, their values are not comparable, and this fact can explain the disparity in the

geometrical parameters calculated for this set of conformers. The reason for this difference between conformers with hydroxyls groups in (*gg*) arrangement and those with OH groups in (*gt*) grouping is due to the fact that the negative hyperconjugation of the lone pairs of the oxygen atoms is favored when both OH groups are disposed in a (*gg*) conformation. In this case, the electronic transfer takes place simultaneously from both oxygen atoms, being the population of the antibonding orbitals $\sigma^*_{Si\text{-}O2}$ and $\sigma^*_{Si\text{-}C4}$ comparable with the population of the antibonding orbitals $\sigma^*_{Si\text{-}O3}$ and $\sigma^*_{Si\text{-}C5}$, respectively. Additionally, when the hydroxyls groups are in (*gt*) disposition, the mentioned electronic transfer from such groups in *trans* arrangement is much weaker. Obviously, this fact has an impact in the observed values of the geometrical parameters of the ten conformers into study.

The magnitude of the interaction between the lone pairs of one of the oxygen atoms and the antibonding SiC and SiO orbitals of each conformer of DESD is shown in Table 3. As shown, the total contribution to the generalized anomeric effect is much higher in conformers in which both hydroxyls groups are arranged in (*gg*) form. The stabilization energy takes, in this set of conformers, an average value of 40.64 kcal/ mol. These results suggest that the (*gg*) conformers are strongly favored and also are consistent with the predicted order of stabilities in the gas phase (I>II>III>IV>V>VI>VII>VIII>IX>X at B3LYP/ aug-cc-pVTZ level) as is discussed below. Moreover, the magnitude of this electronic transfer was also evaluated for the different conformers of DMSD and EMSD, which also confirmed the lower stability of (*gt*) conformers in terms of the generalized anormeric effect.

Table 4 summarize the numerical values of calculated ΔG, ΔG^* and ΔE_0 (see footnote on Table 4 for definition) obtained with the different basis sets used in this work. As shown, the increasing size of the basis set produce a decrease in the difference between the energy values calculated for the set of conformers.

Their relative populations in the gas phase (at room temperature) were calculated theoretically (B3LYP/ aug-cc-pVTZ) from the ΔE_0 values, using the Boltzmann distribution equation. As shown in Figure 3 conformers II, IV, VI and VII have the highest theoretical population in gas phase (14.6%, 14.2%, 11.0% and 10.7%, respectively, at the B3LYP/ aug-cc-pVTZ level). The remaining conformers are calculated to be in lower proportion.

4.2. Vibrational Study

The IR spectra of the solid phase (KBr pellet and thin film) and the Raman spectrum of the pure solid DESD are shown in Figure 4. The observed vibrational bands along with their relative intensities are listed in Table 5 along with their proposed assignments to the normal modes of the main conformers of DESD.

Figure 5 shows a comparison between the theoretical spectra profile (B3LYP/ aug-cc-pVTZ) obtained with the averaged theoretical IR intensities calculated for all the different conformers of DESD (weighted according to their respective Boltzmann populations) and the spectral profile obtained in the same way but considering only the four conformations of lower energy. As can be seen, few differences are found when comparing both theoretical profiles. Thus, the vibrational assignment has been carried out using conformers II, IV, VI and VII as a reference that they represent the 50.5% (B3LYP/ aug-cc-pVTZ) of the total sample composition in gas phase.

4.2.1. High frequency region (3300-1200 cm^{-1})

The theoretical values of the normal modes falling in the 3200-1200 cm^{-1} region reasonably reproduced the experimental profile. However, the theoretical frequencies are deviated from the experimental values as a result of the overestimation caused by the use of the harmonic approximation in the theoretical model.

The IR spectrum of DESD shows a very strong and broad band centered at 3195 cm^{-1} which can be attributed to the stretching of the hydrogen bonded OH groups.

Bands falling in the region between 2970 and 2870 correspond to the CH stretching modes of vibration of both methyl and methylene groups, which have been assigned accordingly to its theoretical values (See Table 5).

Similarly, the experimental bands observed in the 1470-1220 cm^{-1} region have been assigned to the methyl and methylene deformations normal modes according to their theoretical values as reported in Table 5.

4.2.2. Region between 1200-600 cm^{-1}

As expected, the above mentioned experimental-theoretical deviations derived from harmonic character of the theoretically calculated wavenumbers are lower in this region. Nevertheless, the unambiguous assignment of this spectral region is not straightforward, mostly due to the blueshifting of some characteristic vibrational modes of the silanediol group due to hydrogen bonding. As can be seen in Figure 6, the IR spectral profile of the three alkylsilanediols studied (i.e. DMSD, EMSD and DESD) is very similar, mainly in the 1200-1000 cm^{-1} region. The most interesting feature in this spectral region is the presence, in IR spectra of the three systems, of two intense and broad bands that

are not predicted by the theoretical calculations in gas-phase for the respective monomers. Instead, in the case of DMSD [21], theoretical calculations carried out for two hydrogen bonded dimers allow us to justify these experimental features.

IR spectrum of DESD shows a medium intensity band along with a broad band centered at 1172 and 1051 cm^{-1}, respectively. As mentioned above, two similar bands were also found in the IR spectra of DMSD (1176 and 1065 cm^{-1}) and EMSD (1185 and 1060 cm^{-1}). The presence of these bands can be attributed to the -Si-O-H deformation mode of vibration of hydrogen bonded oligomers of different size as was stated in [21] and [22] for the previously studied analogues. This statement is also supported by previous works which study the vibrational spectra of cyclic oligomers of the silanol molecule. [23]

The bands appearing between 1020 and 940 cm^{-1} have been assigned to the C-C stretching mode, CH_3 rocking and CH_2 twisting, according to its theoretical values as reported in Table 6.

The very strong band observed at 879 cm^{-1} has been assigned to the Si-O stretching mode. Considering that the strengthening of the Si-O bond due to the formation of hydrogen bonds produces an increase of *ca.* 20-40 cm^{-1} [24], the medium intensity band centered at 908 cm^{-1} has been attributed to the blueshiftment of the Si-O stretching mode.

In Table 7 are reported the experimental and theoretical bands assigned to the Si-O stretching mode and the blueshifted Si-O stretching mode of the three simplest alkylsilendiols. In view of the results, it could be said that the position of the Si-O stretching mode is affected by the alkyl substitution at the silicon center. Thus, for DMSD [21], we observed that the stretching of the Si-O bond appeared at 904 cm^{-1} (912 cm^{-1}, B3LYP/ aug-cc-pVTZ), and hence the blueshifted Si-O stretching were assigned to a band, also of medium intensity, observed at 949 cm^{-1} (whose theoretical value was calculated at 945 cm^{-1} for the most stable dimer of the molecule in gas-phase). As well, the fundamental Si-O stretching mode of EMSD [22] was assigned to the band centered at 892 cm^{-1} (885 cm^{-1}, B3LYP/ aug-cc-pVTZ), and the blueshifted Si-O stretching was assigned to the shoulder observed at 922 cm^{-1}. As mentioned above, in the case of DESD, the Si-O stretching mode has been assigned to the experimental band centered at 879 cm^{-1} (879 cm^{-1}, B3LYP/aug-cc-pVTZ) and, consequently, the blueshifted Si-O stretching mode has been assigned to the band appearing at 908 cm^{-1}. The general trend of both, experimental and theoretical Si-O stretching mode wavenumber, is to decrease

when moving from the smallest to the biggest alkyl chain. Likewise, the tendency of the blueshifted Si-O stretching mode is also to decrease, since the difference between the fundamental Si-O stretching and the blueshifted band remains *ca.* 40 cm^{-1}. In conclusion, we can say that the Si-O stretching mode is shifted toward lower frequencies when the size of the alkyl substituents is augmented.

The next two bands in the IR spectrum are centered at 855 and 839 cm^{-1}, which have been assigned to the –Si-O-H deformation normal mode of DESD according to its theoretical values.

The experimental bands observed between 800 and 650 cm^{-1} have been assigned to the methylene rocking according to their calculated values. The SiC stretching normal mode appears as a very strong band in the Raman spectrum of the sample centered at 608 cm^{-1}.

4.2.3. Low frequency region

Finally, the spectral region below 600 cm^{-1} has been assigned to the skeletal vibrational modes of the molecule, according to their calculated values. As can be seen in Table 5, considering the presence of different molecular conformations of DESD allowed the tentative assignment of the bands in this region.

5 Conclusions

1. Ten different molecular conformations represent minima on the PES of DESD, which differ in the *anti* or *gauche* (*g*+ or *g*-) orientation of both ethyl groups respect to the Si-O bonds, and depending on the (*gg*) or (*gt*) arrangement of the hydroxyls groups. This conformational diversity derived from the rotation of the Si-C and Si-O bonds of the molecule support the results previously obtained for the analogues DMSD and EMSD.
2. NBO calculations have allowed explaining the predicted order of stabilities in gas phase of the set of conformers into study on the basis of the generalized anomeric effect, being conformers with *gg* arrangement of hydroxyls groups strongly favored since the stabilization energy due to the anomeric effect is twice in such system. These results are also supported by those of the previously studied alkylsilanediols.
3. IR and Raman spectra of DESD have been recorded and completely assigned with the support of the theoretical spectra calculated at the B3LYP/ aug-cc-

pVTZ level. The low frequency region assignment has evidenced the conformational mixture of the samples.

4. It have been seen that the SiO stretching normal mode is affected by the alkyl substitution on silicon center, which is shifted to lower wavenumber as the size of the alkyl substituents is increased. This effect can be seen when the experimental and theoretical values of the Si-O stretching mode of DESD, in this work and those of DMSD and EMSD in references [21] and [22], are compared among them.

6 References

1. Brinker C J, Scherer G W (1989) Sol-Gel Science: The Physics and Chemistry of Sol-Gel Processing. Academic Press, San Diego, CA
2. Mutahi Mw Wa, Nittoli T, Guo L, Sieburth S McN (2002) J Am Chem Soc 124: 7363-7375
3. Nielsen L, Skrydstrup T (2008) J Am Chem Soc 130: 13145-13151
4. George P D, Sommer L H, Whitmore F C (1946) J Am Chem Soc 68: 344-345
5. Kakudo M, Watase T (1953) J Chem Phys Lett 21: 167-168
6. George P D, Sommer L H, Whitmore F C (1953) J Am Chem Soc 75: 1585-1586
7. Tomlins P E, Lydon J E, Akrigg D, Sheldrick B (1985) Acta Cryst. C41: 941-942
8. Cella J A, Carpenter J C (1994) J Organomet Chem 480:23-26
9. Takiguchi T (1959) J Am Chem Soc 81:2359-2361
10. Gaussian 03, Revision E 01, Frisch M J, Trucks G W, Schlegel H B, Scuseria G E, Robb M A, Cheeseman J R, Montgomery J A, Vreven Jr T, Kudin K N, Burant J C, Millam J M, Iyengar S S, Tomasi J, Barone V, Mennucci B, Cossi M, Scalmani G, Rega N, Petersson G A, Nakatsuji H, Hada M, Ehara M, Toyota K, Fukuda R, Hasegawa J, Ishida M, Nakajima T, Honda Y, Kitao O, Nakai H, Klene M, Li X, Knox J E, Hratchian H P, Cross J B, Adamo C, Jaramillo J, Gomperts R, Stratmann R E, Yazyev O, Austin A J, Cammi R, Pomelli C, Ochterski J W, Ayala P Y, Morokuma K, Voth G A, Salvador P, Dannenberg J J, Zakrzewski V G, Dapprich S, Daniels A D, Strain M C, Farkas O, Malick D K, Rabuck A D, Raghavachari K, Foresman J B, Ortiz J V, Cui Q, Baboul A G, Clifford S, Cioslowski J, Stefanov B B, Liu G, Liashenko A, Piskorz P, Komaromi I, Martin R L, Fox D J, Keith T, Al-Laham M A, Peng C Y, Nanayakkara A, Challacombe M, Gill P M W, Johnson B, Chen W, Wong M W, Gonzalez C, Pople J A, Gaussian, Inc, Wallingford CT, 2004

11. Becke A D (1993) J Chem Phys 98:5648-5652
12. Lee C, Yang W, Parr R G (1988) Phys Rev B 37:785-789
13. Hehre W J, Ditchfield R, Pople J A (1972) J Chem Phys 56:2257-2261
14. McLean A D, Chandler G S, J Chem Phys (1980) 72:5639-5648
15. Kendall R A, Dunnning Jr T H, Harrison R J (1992) J Chem Phys 96:6796-6806
16. Fogarasi G, Pulay P (1985) In: Durig, J R (ed) Ab initio calculations of force fields and vibrational spectra. Vibrational Spectra and Structure, 14. Elsevier, New York
17. Sundius T (1990) J Mol Struct 218:321-326
18. Sundius T (2002) Vib Spectrosc 29:89-95
19. Reed A E, Curtiss L A, Weinhold F (1988) Chem Rev 88:899-926
20. Carpenter J E, Weinhold F (1988) J Mol Struct (Theochem) 169:41-62
21. Rodríguez P G, Montejo M, Marchal Ingraín A, Márquez F, López González J J (2012) Vib Spectrosc 58: 79-86
22. Rodríguez P G, Montejo M, Marchal Ingraín A, Márquez F, López González J J (2012) J Sol-Gel Sci Tech 61: 258-267
23. Ignatyev I S, Partal F, López González J J (2002) J Phys Chem A 106: 11644-11652
24. Carteret C (2006) Spectrochim Acta A 64:670-680 (and references therein)

Acknowledgements

The authors thank Andalussian government for funding (FQM173, FQM182) and the CICT facilities of the University of Jaén. P.G.R.O. thanks Spanish Ministerio de Educación for a Ph.D studentship (AP2009-3949) supporting this work.

FIGURE CAPTIONS

Fig. 1 Schematic representation of the so-called (gt) and (gg) arrangement of hydroxyls groups in *gem*-silanediol compounds.

Fig. 2 Molecular structure, atom numbering and point-group symmetries for the ten conformers of diethylsilanediol, DESD.

Fig. 3 Boltzmann's population calculated at the B3LYP/ aug-cc-pVTZ level of theory for the ten conformers of DESD.

Fig. 4 Experimental IR spectra of the sample in KBr pellet (a) and the thin film (b) and the Raman spectrum of the solid phase (c) for DESD.

Fig. 5 Comparison between the theoretical IR spectrum (B3LYP/ aug-cc-pVTZ) calculated considering the weighted contributions of all conformers (a) and those obtained taking into account the weighted contributions of the four main conformers (b).

Fig. 6 Comparison of the experimental IR spectral profile of DMSD (a), EMSD (b), and DESD(c).

Table 1. Main geometrical parameters calculated theoretically (B3LYP/ aug-cc-pVTZ) for conformers of DMSD, EMSD and DESD.[a]

Conformers with (*gg*) arrangement of hydroxyls groups																
	DMSD						EMSD						DESD					
	SiO_2	SiO_3	∠OSiO	SiC_4	SiC_5		SiO_2	SiO_3	∠OSiO	SiC_4	SiC_5		SiO_2	SiO_3	∠OSiO	SiC_4	SiC_5
CI	166.7		110.8	186.8		**CI**	166.7	166.8	110.8	186.9	187.6	**CI**	166.9		110.2	187.6	
						CII	166.8	166.7	110.9	186.9	187.6	**CII**	166.8	166.9	110.6	187.6	187.7
						CII	166.9	166.8	110.5	186.8	187.6	**CIII**	166.8		111.0	187.7	
												CIV	166.8	166.9	110.5	187.7	187.6
												CV	166.8		110.8	187.7	
												CVI	166.8	166.9	111.0	187.9	187.9
Average	166.7		110.8	186.8		**Average**[b]	166.8		110.7	186.9	186.7	**Average**[b]	166.9		110.7	187.6	187.7
												Experimental[c]	163.8	163.6	109.8	184.7	185.2
Conformers with (*gt*) arrangement of hydroxyls groups																	
CI'	166.9	165.9	106.8	186.5	187.7	**CI'**	166.9	166.1	106.8	186.6	188.5	**CVII**	167.0	166.4	109.3	187.1	188.6
						CII'	167.0	165.8	106.0	186.7	188.4	**CVIII**	167.1	166.1	106.1	187.5	188.5
												CIX	167.0	166.0	106.3	187.4	188.6
												CX	166.9	166.6	110.6	187.2	188.8
Average	166.9	165.9	106.8	186.5	187.7	**Average**[d]	166.9	165.9	106.4	186.6	188.4	**Average**[d]	167.0	166.2	108.1	187.3	188.6

[a]Bond distances in pm. Bond angles in degrees. [b]Average of the calculated values for conformers with *gg* arrangement of hydroxyls groups. [c]Experimental data taken form ref. 7. [d]Average of the calculated values for conformers with *gt* arrangement of hydroxyls groups .

Table 2. B3LYP/ aug-cc-pVTZ NBO electronic populations (in a.u.) of the lone pair (LP) orbitals of the oxygen atoms and the σ* orbitals of the SiO and SiC bonds in DESD.

	Electronic population (a.u)									
Orbital	**CI**	**CII**	**CIII**	**CIV**	**CV**	**CVI**	**CVII**	**CVIII**	**CIX**	**CX**
σ SiO_2	1.98457	1.98576	1.98582	1.98562	1.98461	1.98574	1.98554	1.98550	1.98566	1.98551
σ SiO_3	1.98457	1.98576	1.98582	1.98577	1.98468	1.98600	1.98610	1.98618	1.98620	1.98623
σ SiC_4	1.95766	1.95862	1.95857	1.95820	1.95776	1.95884	1.95829	1.95869	1.95853	1.95833
σ SiC_5	1.95766	1.95818	1.95857	1.95848	1.9576	1.95851	1.95963	1.95978	1.95939	1.95968
LP(1)O_2	1.97007	1.96988	1.97004	1.96955	1.97064	1.97085	1.97244	1.97105	1.97018	1.97257
LP(1)O_3	1.97007	1.96974	1.97004	1.97012	1.97064	1.97031	1.96814	1.96927	1.96914	1.96842
LP(2)O_2	1.93727	1.93624	1.93580	1.93611	1.93668	1.93536	1.93481	1.94004	1.93769	1.93354
LP(2)O_3	1.93727	1.93611	1.93580	1.93629	1.93668	1.93579	1.93860	1.93778	1.93769	1.93788
σ* SiO_2	0.07868	0.07325	0.07379	0.07233	0.07609	0.06924	0.06856	0.06654	0.06795	0.06693
σ* SiO_3	0.07868	0.07648	0.07379	0.07726	0.07609	0.07767	0.07076	0.06303	0.05744	0.07727
σ* SiC_4	0.06216	0.05896	0.06153	0.06362	0.06423	0.06114	0.05827	0.06635	0.06451	0.05372
σ* SiC_5	0.06216	0.06338	0.06153	0.06009	0.06423	0.06273	0.07150	0.07085	0.07411	0.07066

Table 3. Magnitude (in kcal·mol^{-1}) of the interaction energies between the two lone pairs orbitals of the oxygen atoms and the σ* orbitals of the SiC and SiO bonds in DESD calculated at the B3LYP/ aug-cc-pVTZ level.

	$E^{(2)}$ (kcal mol^{-1})									
interaction	**CI**	**CII**	**CIII**	**CIV**	**CV**	**CVI**	**CVII**	**CVIII**	**CIX**	**CX**
LP(1) O_2→σ* SiO_3	1.31	1.26	0.92	1.10	1.15	0.86	-	2.20	2.44	-
LP(1) O_3→σ* SiO_2	1.31	096	0.92	1.34	1.15	1.08	2.69	2.65	2.04	1.80
LP(1) O_2→σ* SiC_4	1.93	1.91	2.18	2.18	2.16	2.28	1.11	-	-	1.60
LP(1) O_3→σ* SiC_4	2.99	3.00	3.02	3.04	3.07	3.11	2.96	2.74	2.98	3.24
LP(1) O_2→σ* SiC_5	2.99	3.01	3.02	3.01	3.07	2.97	3.49	3.36	3.39	3.27
LP(1) O_3→σ* SiC_5	1.93	2.21	2.18	1.92	2.16	2.12	0.90	0.74	1.05	1.45
LP(2) O_2→σ* SiO_3	8.84	9.06	9.76	9.40	9.29	9.95	9.81	4.95	4.10	10.92
LP(2) O_3→σ* SiO_2	8.84	9.57	9.76	8.78	9.29	9.29	5.84	4.97	2.04	7.72
LP(2) O_2→σ* SiC_4	5.34	5.00	4.31	4.84	4.76	4.08	4.27	7.61	7.68	2.83
LP(2) O_3→σ* SiC_4	-	-	-	-	-	-	0.72	1.01	-	-
LP(2) O_2→σ* SiC_5	-	-	-	-	-	-	-	0.95	1.44	0.56
LP(2) O_3→σ* SiC_5	5.34	4.63	4.31	5.18	4.76	4.62	7.16	7.58	6.85	6.01
∑	**40.82**	**40.61**	**40.38**	**40.79**	**40.86**	**40.36**	**38.95**	**38.76**	**34.01**	**39.40**

Table 4. Relative Gibbs free energies (G and G*)[a] and E_0[b] Energies of the ten conformers of DESD calculated at the B3LYP level in conjunction with the different basis sets employed. Energy values in kcal·mol.

		ΔG (kcal mol^{-1})			ΔG* (kcal mol^{-1})			ΔE$_o$ (kcal mol^{-1})		
		6-31G*	6-31++G**	aug-cc-pVTZ	6-31G*	6-31++G**	aug-cc-pVTZ	6-31G*	6-31++G**	aug-cc-pVTZ
B3LYP	I	0,19	0,42	0,31	1,14	1,19	1,19	0.00	0.00	0.00
	II	0,00	0,14	0,00	0,00	0,00	0,00	0.15	0.10	0.07
	III	0,54	0,61	0,00	0,48	0,43	0,00	0.22	0.10	0.07
	IV	0,01	0,21	0,07	0,08	0,05	0,07	0.21	0.16	0.14
	V	0,68	0,79	0,59	0,69	0,55	0,56	0.38	0.23	0.18
	VI	0,58	0,81	0,62	0,75	0,64	0,66	0.91	0.79	0.76
	VII	0,94	0,00	0,25	1,93	1,60	1,32	1.49	1.00	0.84
	VIII	0,72	0,85	0,59	1,78	1,39	1,21	1.36	0.00	0.95
	IX	1,03	1,03	0,64	2,10	1,76	1,54	1.66	1.33	0.12
	X	1,49	1,43	1,09	2,51	2,10	1,89	2.11	1.78	1.58

[a]ΔG* stands for the Gibbs free energy values obtained when the entropic corrections to the low frequency modes of vibrations are subtracted from the Gibbs free energies calculated. [b]$E_0 = E_e + ZPE$.

Table 5. Experimentally observed bands (with relative intensities) and theoretical frequencies (in cm^{-1}) calculated at the B3LYP/ aug-cc-pVTZ level for conformers of DESD and the proposed assignments.

Experiment[a]							
IR		**Raman**	**Theory**				
KBr pellet	**Thin film**	**Solid**	**CII**	**CIV**	**CVI**	**CVII**	**Assignment**[b,c]
			3874	3873	3873	3891	νOH
			3872	3871	3871	3880	
3195 vs, br	3180 vs, br						νOH network
2966 vs	2966 vs	2967 vs	3092	3090	3097	3088	ν^{as} CH_3
2955 vs	2956 vs	2958 m	3090	3084	3087	3084	
2937 vs	2938 vs	2938 m	3074	3076	3079	3076	
			3069	3070	3076	3074	
2911 vs	2911 s	2912 s	3046	3041	3040	3049	ν^{as} CH_2
			3039	3045	3035	3030	
2892 vs	2892 s	2893 s	3024	3023	3028	3024	ν^{s} CH_3
			3020	3020	3025	3022	
2876 vs	2876 s	2877 s	3015	3015	3009	3020	ν^{s} CH_2
			3008	3012	3003	2998	
2804 sh, w	2809 w	2806 vw					Overtone(2x1414)
2736 vw	2734 vw	2735 w					Overtone(2x1374)
2678 vw	2681 vw						Combination(1453+1248)
1470 m	1469 w	1471 m	1510	1510	1512	1510	δ^{as} CH_3
			1508	1508	1508	1507	
1453 m	1453 w	1454 m	1504	1504	1505	1505	δ^{as} CH_3
			1504	1504	1500	1503	
1414 m	1414 m	1416 m	1455	1455	1457	1456	sc CH_2
			1452	1454	1450	1453	
1374 w	1373 w	1375 vw	1416	1418	1421	1416	δ^{s} CH_3
			1414	1413	1414	1415	
1248 m	1248 sh, m	1249 vw	1283	1282	1284	1280	wa CH_2
1240 m	1240 m		1276	1276	1278	1275	
1229 w	1229 w	1234 vw	1270	1269	1270	1267	tw CH_2 + ρ CH_3
			1266	1262	1262	1262	
1172 m	1172 m,br						Oligomers[d]
1050 m	1051 m						
1017 s	1017 m	1018 w	1033	1033	1039	1031	ν CC + ρ CH_3
1012 s	1012 m		1025	1025	1026	1029	ν CC + ρ CH_3
978 sh, m	978 sh, m	973 w	992	989	999	986	tw CH_2 + ν CC
970 m	969 m	962 w	984	985	985	985	ν CC + ρ CH_3 + tw CH_2
947 sh, m	948 sh, w		977	976	983	974	ρ CH_3 + ν CC + tw CH_2
942 m	942 m		968	968	963	967	ρ CH_3 + tw CH_2
908 m	908 w						ν SiO blueshifted
879 vs	878 vs	874 vw	879	879	881	891	ν SiO + δ SiOH
855 vs	857 vs	850 vw	874	874	869	877	δ SiOH + ν SiO
839 sh, vs	840 sh, w		853	855	858	820	
745 s	745 s	743 vw	790	788	788	788	ν SiO + δ SiOH
720 sh, m	722 sh, m		711	716	714	711	ρ CH_2 + ν SiC
698 m		697 vw	699	696	702	703	ρ CH_2
660 w	661 w		676	671	656	670	ρ CH_2 + ν SiC
607 w		608 vs	598	598	590	586	ν SiC
				404	410		wa CSiC+ sc CCSi
387 m		381 w	397			375	sc CCSi + wa CSiC
357 m		356 w	362	369	350	362	sc OSiO + τ SiO
		346sh, w	333				wa CSiC + ρ SiC_2

333 m		331 vw		325			ρ SiC_2 + wa CSiC
					314		wa CSiC+scCCSi
			288	286	287	288	τCC + scCSiC (ρ SiC_2)
					279		tw SiC_2+scCSiC+scCCSi
					243		τ SiO
		257 vw	254	260		251	τ CC + tw SiC_2
		230 vw	230	231	230		τ SiO + sc OSiO
			231	234			
			192	190	192	203	τCC +scCCSi + wa CSiC
							scCCSi+τSiO
		168 vw	178	179	164	174	scCCSi+scCSiC+ ρ SiC_2
			157	151	156	159	scCCSi + ρSiC_2 + twSiC_2
					138	148	scCSiC+ρ SiC_2+scCCSi
						123	twSiO_2 + scCSiC
		105 vw	115	117			sc CSiC (sc CCSi)
						84	τSiO + scOSiO
					71	73	τSiC+τSiO + scOSiO
			61	60			τSiC
			54	55		50	
					36		

[a]Abrevations: vs= very strong, s= strong, m=medium, w=weak, vw=very weak, sh= shoulder, br= broad. [b]Only shown contributions higher than 15%. [c]Symbols used: ν= stretching, δ= deformation, ρ= rocking, τ= torsion, sc= scissoring, tw= twisting, wa= wagging. Superscripts "s" and "as" denote symmetric and asymmetric motions. [d]See text for explanation.

Table 6. Comparison between the experimental and theoretical (B3LYP/ aug-cc-pVTZ) frequency values of the Si-O stretching mode obtained for DMSD (dimethylsilanediol), EMSD (ethylmethylsilanediol) and DESD (diethylsilanediol).

		Frequency (cm^{-1})		
		DMSD	**EMSD**	**DESD**
ν SiO	Experiment	928	892	879
	Theory[a.b]	916	885	879
ν SiO blueshifted	Experiment	949	922	908
	Theory	945[c]	-	-

[a]Theoretical values calculated at the B3LYP/ aug-cc-pVTZ. [b]Theoretical values reported correspond to those of the most stable molecular conformations of each system. [c]Value obtained for the most stable theoretical dimer of DMSD.

Figure 1
Click here to download high resolution image

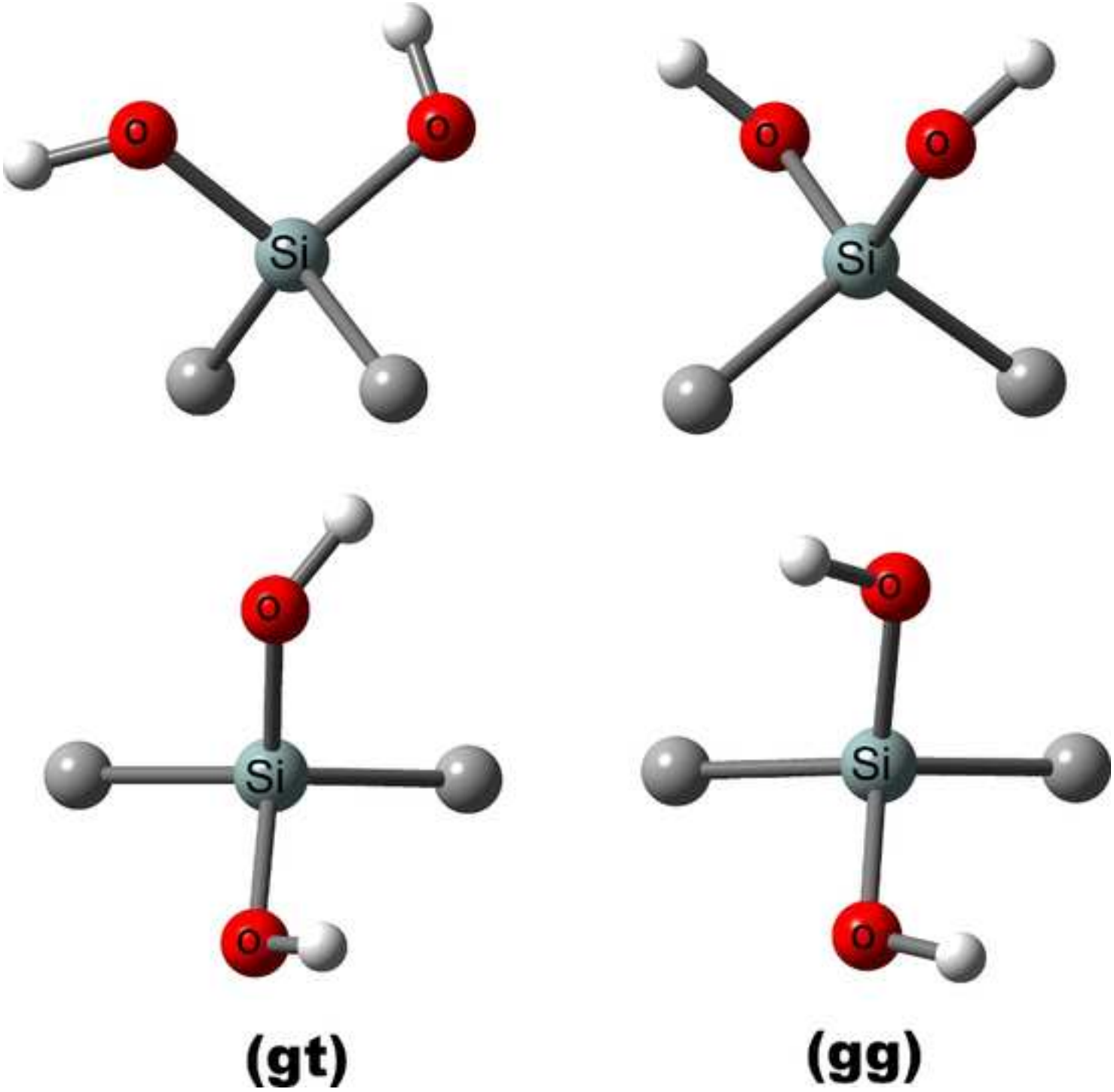

Figure 2
Click here to download high resolution image

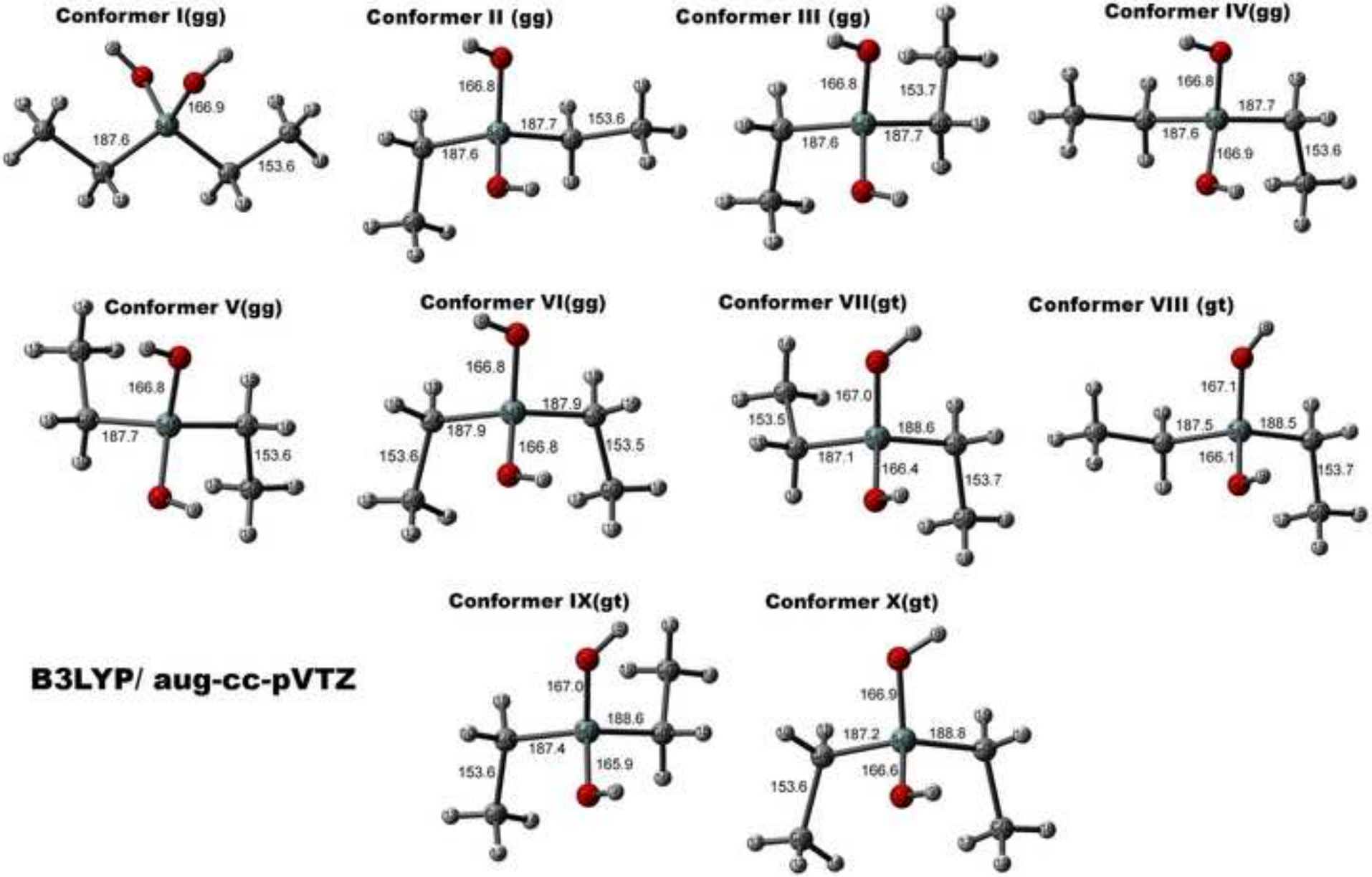

Figure 3
Click here to download high resolution image

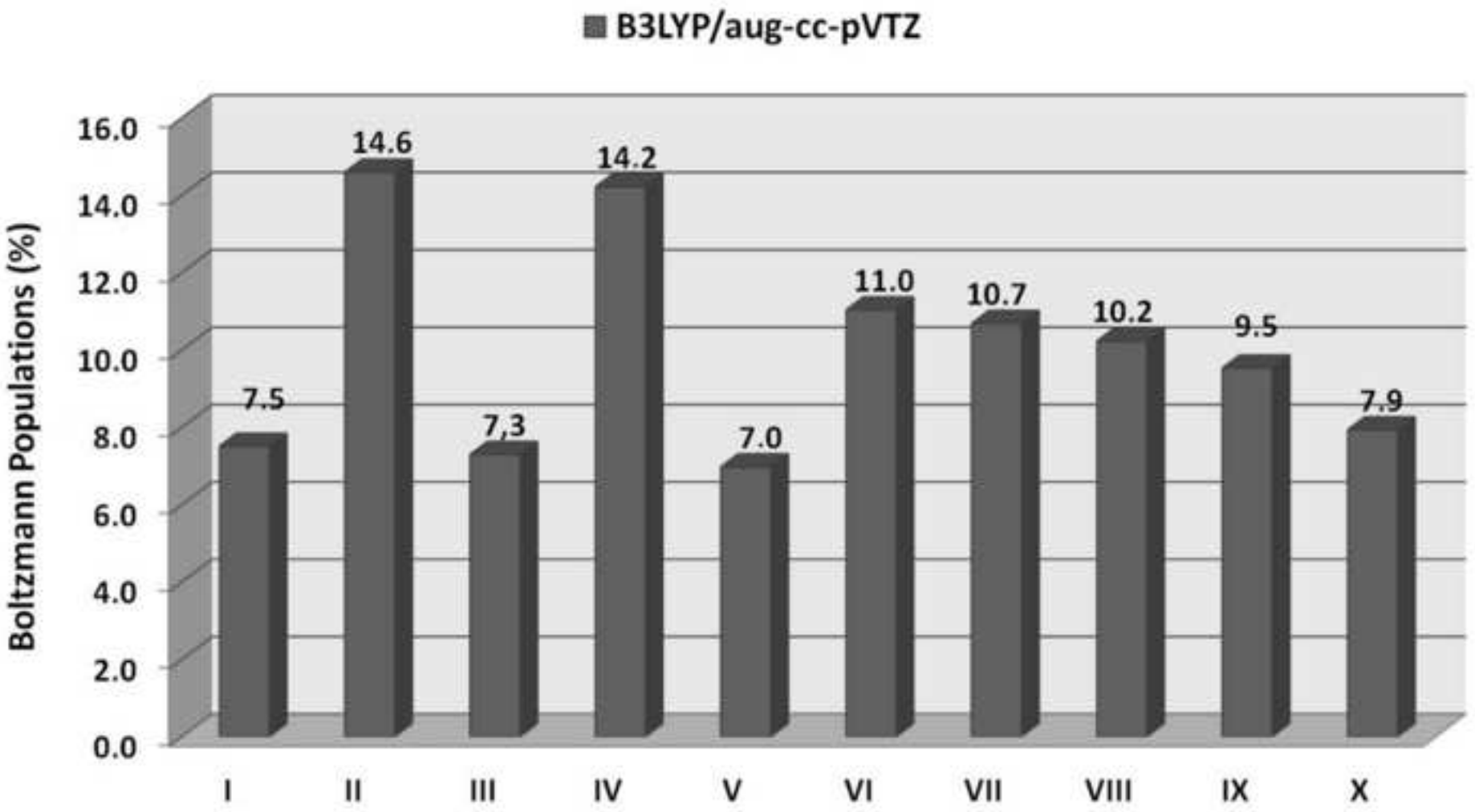

Figure 4
Click here to download high resolution image

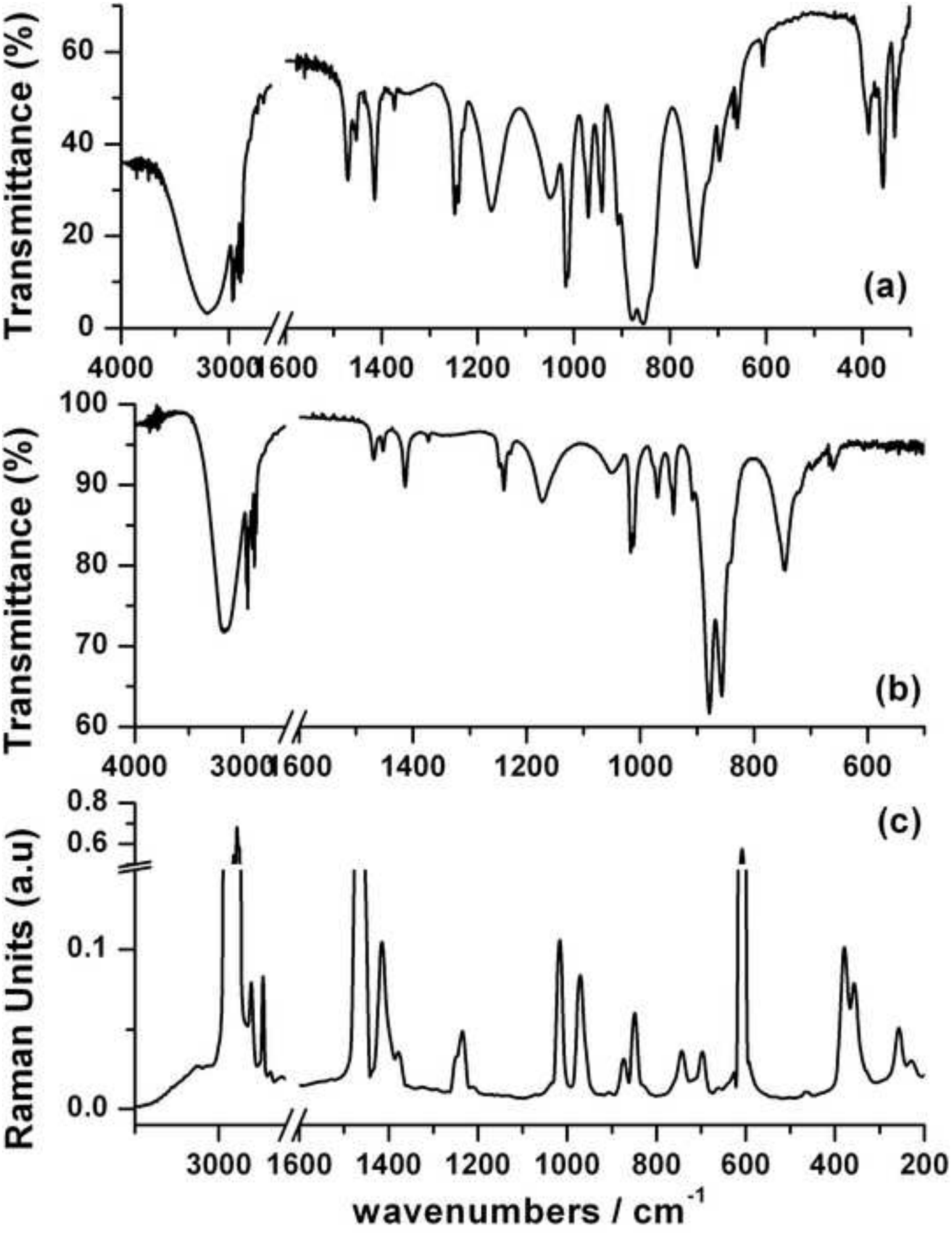

Figure 5
Click here to download high resolution image

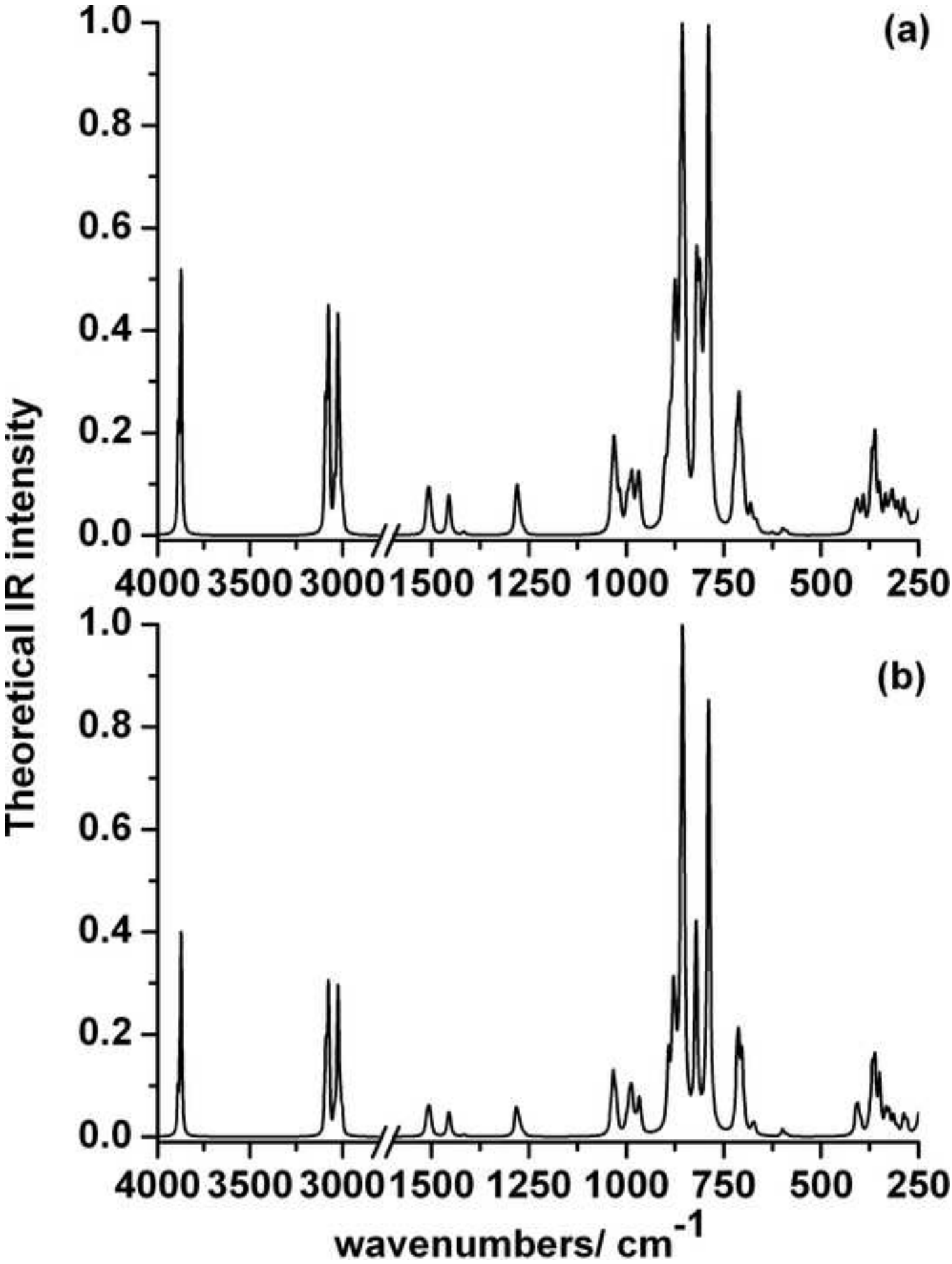

Figure 6
Click here to download high resolution image